Biexciton binding energy in CuCl quantum dots

doi: 10.1103/PhysRevB.50.18658

Biexciton binding energy in CuCl quantum dots

Yasuaki Masumoto, Shinji Okamoto, and Satoshi Katayanagi
Institute of Physics, University of Tsukuba, Tsukuba 305, Japan
(Received 23 May 1994; revised manuscript received 18 July 1994)

Induced absorption from the exciton state to the biexciton state was clearly observed under the site-selective excitation of the inhomogeneously broadened Z_3 exciton band in CuCl microcrystallites embedded in NaCl crystals. This allows us to obtain the size-dependent biexciton binding energy in CuCl quantum dots. The binding energy of biexcitons increases with the decrease in their size and its size dependence and bulk value are well represented by the expression $78/a^{*2}+52/a^{*}+33$ (meV), where a^{*} is the effective radius of microcrystallites in a unit of nm. The experimental results are compared with an available theoretical result. The enhanced Coulomb interaction in microcrystallites still increases the biexciton binding energy in the large-size regime, where the quantum confinement energy of excitons is not considerable. The size-dependent biexciton binding energy cannot be explained by the weak-confinement model of biexcitons.

It is well established that the quantum confinement effect in semiconductor microcrystallites (quantum dots) is classified into the weak confinement regime and the strong confinement regime.[1-3] In the weak confinement regime, the exciton center-of-mass translational motion is quantized and the blueshift of the exciton energy is expressed as $\pi^2\hbar^2/2M(a-a_B/2)^2$, where M is the translational mass of the exciton, a is the radius of microcrystallites, and a_B is the Bohr radius of the exciton.[2] Here the so-called dead-layer correction is included as $a-a_B/2$, and we use $a^{*}=a-a_B/2$, the effective radius, in the following text. In this regime, one may consider that the center-of-mass translational motion of the biexciton is also quantized.[4] Because the biexciton translational mass is about twice the exciton translational mass, the biexciton binding energy is expected to increase by $\pi^2\hbar^2/4Ma^{*2}$ with decrease of the radius. Theoretically, the biexciton state in the weak confinement regime has been treated by using this simple expression.[5] However, the experimental results for CuCl quantum dots, which are the prototypical material belonging to the weak confinement category, are confused and do not follow this simple relation.[4,6] In the case of CuCl microcrystallites in NaCl crystals, the biexciton luminescence varies with the change of the size of microcrystallites,[4] but does not vary in the case of CuCl microcrystallites in glass.[6] In the former case, the biexciton binding energy seems to vary by $\pi^2\hbar^2/4Ma^{*2}$ from the large-size limit of microcrystallites. However, the reported biexciton binding energy of the CuCl microcrystallites at the large-size limit, 42 meV, does not agree with that of bulk CuCl, 33 meV.

Obviously, the experimental determination of size-dependent biexciton binding energy has been obstructed by the size inhomogeneity of quantum dots. In the weak confinement regime, the exciton blueshift is proportional to $1/a^{*2}$, so that site-selective spectroscopy was used to overcome this difficulty. However, site-selective luminescence spectroscopy did not succeed in observation of single-size microscrystallites, because the higher excited states of large microcrystallites are superposed on the ground states of small microcrystallites and because the biexciton luminescence is stronger in larger microcrystallites.[4] In fact, luminescence spectra of CuCl quantum dots under site-selective excitation give small biexciton structures which move with the change of the excitation photon energy, while the moving structures are much smaller than the nonmoving biexciton luminescence band coming from the large microcrystallites.[4] This makes it bothersome to obtain size-dependent biexciton binding energy.

In this study, we used the nanosecond pump-and-probe method under the site-selective excitation. The burnt hole in the exciton absorption band and the induced absorption band were studied as a function of the excitation photon energy. The induced absorption band arises from the transition from the transverse exciton state to the biexciton state. By observing both the induced absorption band and the burnt hole with the change in the pump photon energy, we can obtain the biexciton binding energy as a function of the size of quantum dots. The site-selective pump-and-probe method is superior to the site-selective luminescence method, because the former is not affected by the size-dependent luminescence yield of excitons and biexcitons.

Samples studied in this work are CuCl microcrystallites in NaCl crystals and a platelet-type CuCl single crystal 18 μm thick. The preparation and characterization procedures of microcrystalline samples were written in our previous papers.[7,8] The average size of microcrystallites was determined by small-angle x-ray-scattering measurement. Samples were directly immersed in superfluid helium and were studied in a nanosecond pump-and-probe configuration. For the microcrystalline samples, a narrow-band dye laser (Lumonics HD500) pumped by a 30-Hz Q-switched Nd^{3+}:YAG (yttrium aluminum garnet) laser was the pump source. For the bulk sample, the third harmonics of the Nd^{3+}:YAG laser were used as the pump source. In both cases, probe pulses were amplified spontaneous emission of LD390 dye pumped by the same Nd^{3+}:YAG laser. The linewidth of the dye pump pulses was 0.014 meV, which is narrower than the homogeneous linewidth of Z_3 excitons in CuCl microcrystallites.[8] The

pump-and-probe spectra were measured by a diode-array-type optical multichannel analyzer and a 93-cm monochromator with a spectral resolution of 0.6 meV. The luminescence spectrum was also studied at 77 K under the excitation of the third harmonics of the Nd^{3+}:YAG laser.

Pump-and-probe spectra are shown in Fig. 1. The spectra of the microcrystalline sample consist of the bleaching structure of Z_3 excitons which is burnt out by the spectrally narrow pump pulses, and the induced absorption structure due to the transition from the transverse exciton state to the biexciton state. Burnt holes in the exciton absorption spectra move with the change in the pump photon energy. Simultaneously, the induced absorption band shows the energy shift, but it is much smaller than the pump energy shift. Burnt holes are the main part in the bleaching structure in the Z_3 exciton absorption band. Therefore, the burnt exciton state is relevant to the induced absorption band. The induced absorption band and the burnt holes are observed simultaneously by nanosecond pump-and-probe spectroscopy. This means that they are directly connected with each other. The situation is different in the case of luminescence spectroscopy under the site-selective excitation, because the biexciton luminescence decay time (80 ps) is much faster than the exciton luminescence decay time (1.6 ns).[7] In this sense, it is difficult to connect the exciton luminescence band with the biexciton luminescence band directly. The induced absorption band due to the transition from the transverse exciton state to the biexciton state in bulk CuCl is also shown in Fig. 1. It was observed at 3.169 eV, in agreement with the previous report.[9,10] This means that the biexciton binding energy in bulk CuCl is 33 meV.

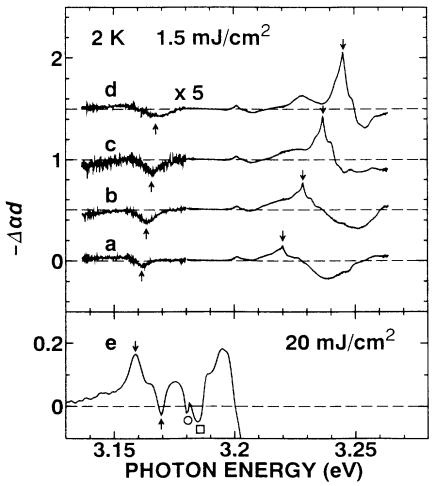

FIG. 1. Differential absorption spectra of CuCl microcrystallites under the site-selective excitation. The average radius of CuCl microcrystallites in the sample was 2.7 nm, and the sample had a broad size distribution of microcrystallites. The excitation photon energy for (a), (b), (c), and (d) is 3.2204, 3.2288, 3.2372, and 3.2457 eV, respectively. Downward arrows show the burnt hole in the inhomogeneously broadened exciton band, while upward arrows show the induced absorption coming from the transition from the exciton state to the biexciton state. The exciton density was 1.5 mJ/cm^2. The differential absorption spectrum of a CuCl bulk crystal under the band-to-band excitation is also shown at the bottom part (e). The excitation photon energy was 3.49 eV, and its density was 20 mJ/cm^2. The upward arrow shows the induced absorption, the downward arrow the optical gain maximum, the open circle the I_1 bound exciton, and the open square the two-photon absorption of biexcitons.

In Fig. 2 the energy position of the induced absorption band is plotted as a function of the pump photon energy, which is exactly equal to the burnt exciton energy. The energy of the induced absorption band increases slowly and monotonously with the increase in the pump photon energy. It is noted that the blueshift of the induced absorption is much smaller than that of the burnt hole in the exciton band. The energy of the induced absorption band for the bulk sample was also indicated in Fig. 2.

The biexciton binding energy B_{xx} is defined as $B_{xx}=2E_x-E_{xx}$, where E_x is the exciton energy and E_{xx} the biexciton energy. The transition from the exciton to the biexciton takes place at $E_{xx}-E_x$, which corresponds to the induced absorption band. Therefore, the biexciton binding energy B_{xx} is obtained by the burnt exciton energy E_x minus the induced absorption energy, $E_{xx}-E_x$. We can obtain the biexciton binding energy readily from Fig. 2. The blueshift of the quantized exciton energy ΔE is related to the effective radius of CuCl microcrystallites a^* as $\Delta E=\pi^2\hbar^2/2Ma^{*2}$.[11] In this way, the biexciton binding energy is obtained in Fig. 3 as a function of the effective radius of microcrystallites.

So far, the biexciton binding energy in semiconductor quantum dots has been a subject of extensive theoretical study. Because a biexciton is a composite of two electrons and two holes, we must solve the four-body problem under the spatially restricted condition. The perturbation method,[12,13] the variational method,[5,14,15] the matrix-diagonalization method,[16,17] and the path-integral method[18] were used to calculate the binding energy of the biexciton. The most sophisticated variational result differs much from the matrix-diagonalization result at the small-radius limit.[15,17] Because two electrons and two holes are spatially confined in a small quantum dot, both Coulomb attraction between electrons and holes and Coulomb repulsion between two electrons (holes) are much enhanced simultaneously with the increase of kinetic energy due to the spatial localization. This competition brought forth the controversial results. A weak

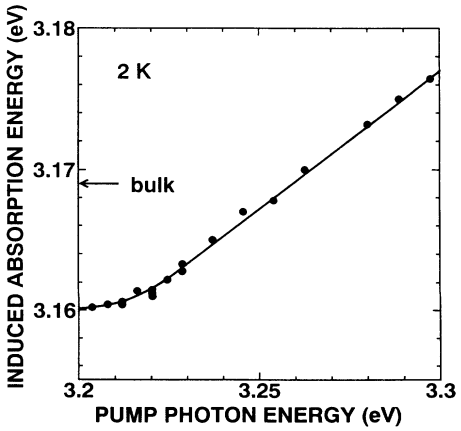

FIG. 2. Induced absorption energy as a function of the pump photon energy. The energy of the induced absorption band in bulk CuCl is shown by an arrow. The solid line is a guide for eyes.

point of the variational approach is that one of the variational parameters is fixed. On the other hand, the numerical matrix-diagonalization method seems not to have a weak point at the small-size regime,[19] and gives a functional form to the biexciton binding energy. The biexciton binding energy is expressed by $B_{xx}=C_1/a^2+C_2/a+B_{xx}$(bulk), where C_1 and C_2 are independent of the radius and B_{xx}(bulk) is the biexciton binding energy in the bulk crystal.

Other variational approaches to the biexciton binding energy in a quantum dot are based on the adiabatic approximation or two-body approximation.[5,14] They used smaller numbers of variational parameters than Ref. 15 to calculate the biexciton binding energy. They are too simple to derive the biexciton binding energy in quantum dots, because the competition among Coulomb attraction energy, Coulomb repulsion energy, and kinetic energy is quite delicate. Another reason why we do not use the calculation of Ref. 5 is that it derives the expression of biexciton binding energy $B_{xx}=\pi^2\hbar^2/4Ma^{*2}+B_{xx}$(bulk) at the large-size limit, because the expression conflicts with our experimental results as described below. In this paper, therefore, we compared our experimental results with the calculated result done by the numerical matrix-diagonalization method,[16,17] although the calculated result is limited within the rather small-radius range $a<5a_B$. The calculated result is shown by a dashed line in Fig. 3. In the calculation, we replaced a by a^*. Here we used the well-known CuCl parameters, an exciton binding energy of 213 meV, and an exciton Bohr radius of 0.68 nm. Therefore, the calculated range is limited up to $5a_B=3.4$ nm. The calculated binding energy is a little smaller than the experimental data, but the overall radius dependence is the same. It is noted that the calculation was done with the condition $m_e^*/m_h^*=0.2$ and $\varepsilon_1/\varepsilon_2=1$, where $m_{e(h)}^*$ is the effective mass of the electron (hole), and ε_1 and ε_2 are dielectric constants of the quantum dots and matrix, respectively. The dielectric constant of CuCl is $\varepsilon_1=7.9$,[20] while that of NaCl is $\varepsilon_2=5.6$. The ratio $\varepsilon_1/\varepsilon_2$ is 1.4. In this case, the dielectric confinement effect makes the enhancement curve of the biexciton binding energy steeper.[15,21] The disagreement between the experimental data and the theoretical curve is reduced by taking account of the dielectric confinement effect.

Experimental data in Fig. 2 and the solid circles in Fig. 3 suggest that the biexciton binding energy seems to approach 42 meV at the large-size limit, if the biexciton binding energy in a bulk crystal is not taken into account. In fact, we can fit the experimental solid circle data in Fig. 3 by using the expression $C/a^{*2}+42$ (meV), where the functional form is based on the weak confinement model of biexcitons. The value, 42 meV, is larger than the biexciton binding energy in bulk CuCl, 33 meV, by 9 meV. The biexciton binding energy should approach the bulk value at the large-size limit. At the large-size regime, the relation between the radius of microcrystallites and the blueshift of the exciton energy is not necessarily held.[22] This probably obscured the clear observation of the size-dependent biexciton binding energy at the large-size regime. The approach of the biexciton binding energy to the bulk value was seen in the biexciton luminescence spectra of samples which contain different average-size CuCl microcrystallites. Figure 4 shows the luminescence spectra of microcrystallite and bulk samples under the band-to-band excitation. The luminescence band observed around 3.17 eV comes from the biexciton annihilation, leaving the longitudinal exciton behind. The biexciton luminescence energy of CuCl microcrystallites whose radius is less than 5.4 nm is lower than that in the bulk sample by 7.5 meV. However, the biexciton luminescence energy of 9.5-nm CuCl microcrystallites goes to higher energy and is close to the bulk energy.

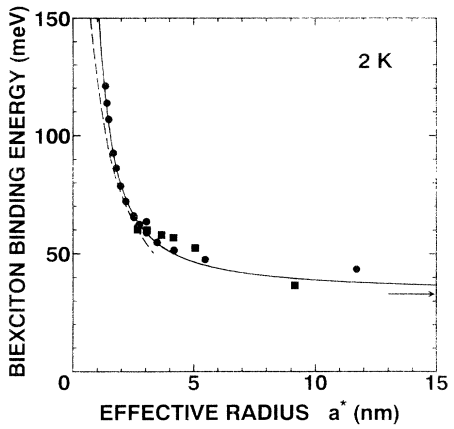

FIG. 3. Biexciton binding energy as a function of the effective radius of CuCl microcrystallites. The effective radius is defined by $a^*=a-a_B/2$. Solid circles are obtained by the induced absorption energy, and solid squares are obtained by the biexciton luminescence energy. Biexciton binding energy in bulk CuCl is shown by an arrow. A solid line is a phenomenological curve fitted by the expression $78/a^{*2}+52/a^*+33$ (meV), where a^* is the effective radius in a unit of nm. A dashed line is based on the calculation done by Hu, Lindberg, and Koch, with parameters $m_e^*/m_h^*=0.2$ and $\varepsilon_1/\varepsilon_2=1$.

This observation shows that biexciton binding energy varies much more than the quantized energy of the exciton center-of-mass translational motion at the large-size regime. It means the failure of the model,[4,5] which assumes that biexciton center-of-mass translational motion is quantized in CuCl microcrystallites at the large-size limit. One cannot fit the experimental data including the bulk data in Fig. 3 at the large-size limit by taking the expression $C/a^{*2}+33$ (meV). Instead, the experimental results were fitted fairly well by the expression $B_{xx}=C_1/a^{*2}+C_2/a^*+33$ (meV), and $C_1=78$ and $C_2=52$ were obtained, where a^* is in units of nm. The important contribution of the C_2/a^* term suggests the significant contribution of the Coulomb term at the large-size regime.

The quantum-size effect for not only biexciton binding energy but also bound exciton binding energy was discussed in the quantum well.[23] Both of them increase with the decrease in the well thickness. Figure 4 shows the bound exciton luminescence I_1 and I_2 of CuCl microcrystallites, and their energies increase with the increase in the size from 5.4 to 9.5 nm. The I_1 line comes from the exciton bound to the neutral acceptor, and the I_2 line comes from the exciton bound by a neutral donor.[10] It is well known that the Hamiltonian for the exciton bound by a neutral donor or a neutral acceptor is similar to that

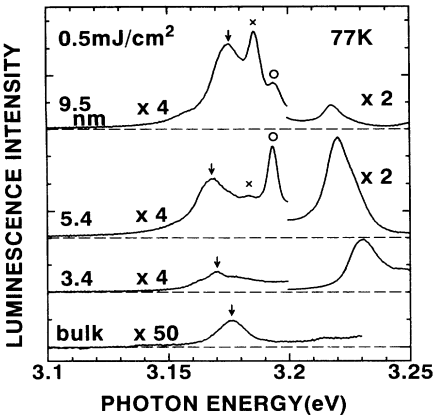

FIG. 4. Luminescence spectra of different-size CuCl microcrystallites and a bulk CuCl crystal. The excitation photon energy was 3.49 eV, and its density was 0.5 mJ/cm^2. Downward arrows show the biexciton luminescence, open circles I_1 bound exciton luminescence, and crosses I_2 bound exciton luminescence. The mean radius shown was estimated by the small-angle x-ray-scattering experiment.

for the biexciton. The Hamiltonian comes from the kinetic-energy term and the Coulomb energy term. The Coulomb energy term among two electrons and two holes is common in both excitons bound by a neutral donor (acceptor) and a biexciton, and the difference arises in the kinetic-energy term. The contribution of the kinetic-energy term to the enhancement of the binding energy is smaller than the observed enhancement of the binding energy. In fact, $\pi^2\hbar^2/4Ma^{*2}=3.0$ meV is much smaller than the observed enhancement of the binding energy, 19.5 meV, at $a^*=5.1$ nm. Therefore the similar energy shift of biexciton and bound excitons at the large-size regime is ascribed to the significant contribution of the Coulomb energy term. The enhancement of the biexciton binding energy at the large-size regime is interpreted in this way. At the large-size regime, the Coulomb energy still grows with the increase in the size of microcrystallites. Biexciton diameter in CuCl is 3 nm and the extent is not much smaller than even 10 nm. Because the exciton binding energy is as large as 213 meV, the increase in the biexciton binding energy is not negligible even with the slight reduction of the size.

In summary, induced absorption from the exciton state to the biexciton state was clearly observed under the site-selective excitation of the inhomogeneously broadened Z_3 exciton band in CuCl microcrystallites embedded in NaCl crystals. This allows us to obtain the size-dependent biexciton binding energy in CuCl quantum dots. The binding energy of biexcitons increases with the decrease in the size, and its size dependence was well fitted by the expression $78/a^{*2}+52/a^*+33$ (meV), where a^* is the effective radius of microcrystallites in units of nm. The experimental results are fairly well explained by the theoretical result by Hu *et al.*[16,17] It is noted that biexciton binding energy still increases at the large-size regime, where the quantum confinement energy of the exciton is not considerable. Biexciton binding energy cannot be explained by the weak confinement model of biexcitons, where center-of-mass translational motion of biexcitons is quantized. Coulomb interaction still increases the binding energy of biexcitons in the large-size regime.

Small-angle x-ray-scattering experiments were done by the approval of the Photon Factory (PF) Advisory Committee (Proposal 92-117). The authors wish to thank Professor Y. Amemiya of PF for his kind guidance to the small-angle x-ray-scattering experiments. This work was supported by the New Energy and Industrial Technology Development Organization (NEDO) of Japan.

[1]A. I. Ekimov, Al. L. Efros, and A. A. Onushchenko, Solid State Commun. **56**, 921 (1985).
[2]Y. Kayanuma, Phys. Rev. B **38**, 9797 (1988).
[3]A. D. Yoffe, Adv. Phys. **42**, 173 (1993).
[4]T. Itoh, F. Jin, Y. Iwabuchi, and T. Ikehara, in *Nonlinear Optics of Organics and Semiconductors,* edited by T. Kobayashi (Springer, Berlin, 1989), p. 76.
[5]Y. Kayanuma and K. Kuroda, Appl. Phys. A **53**, 475 (1991).
[6]R. Levy, L. Mager, P. Gilliot, and B. Hönerlage, Phys. Rev. B **44**, 11 286 (1991).
[7]Y. Masumoto, T. Katayanagi, and T. Mishina, Phys. Rev. B **49**, 10 782 (1994).
[8]T. Wamura, Y. Masumoto, and T. Kawamura, Appl. Phys. Lett. **59**, 1758 (1991).
[9]Y. Masumoto and S. Shionoya, J. Phys. Soc. Jpn. **51**, 181 (1982).
[10]M. Ueta, H. Kanzaki, K. Kobayashi, T. Toyozawa, and E. Hanamura, *Excitonic Processes in Solids* (Springer, Berlin, 1986), Chap. 3.
[11]T. Itoh, Y. Iwabuchi, and M. Kataoka, Phys. Status Solidi B **145**, 567 (1988).
[12]L. Banyai, Y. Z. Hu, M. Lindberg, and S. W. Koch, Phys. Rev. B **38**, 8142 (1988).
[13]L. Banyai, Phys. Rev. B **39**, 8022 (1989).
[14]Al. L. Efros and A. V. Rodina, Solid State Commun. **72**, 645 (1989).
[15]T. Takagahara, Phys. Rev. B **39**, 10 206 (1989).
[16]Y. Z. Hu, S. W. Koch, M. Lindberg, N. Peyghambarian, E. L. Pollock, and F. F. Abraham, Phys. Rev. Lett. **64**, 1805 (1990).
[17]Y. Z. Hu, M. Lindberg, and S. W. Koch, Phys. Rev. B **42**, 1713 (1990).
[18]E. L. Pollock and S. W. Koch, J. Chem. Phys. **94**, 6776 (1991).
[19]The numerical matrix-diagonalization method is not reliable at the large-size regime, because the increased number of basis functions is too many to be treated computationally. As a result, Ref. 17 restricts the calculation range to $a < 5a_B$.
[20]*Numerical Data and Functional Relationships in Science and Technology (Physics of II-VI and I-VII Compounds, Semimagnetic Semiconductors),* edited by O. Madelung, Landolt-Börnstein, New Series, Group III, Vol. 17, Pt. b (Springer-Verlag, Berlin, 1982).
[21]Y. Z. Hu, S. W. Koch, and D. B. Tran Thoai, Mod. Phys. Lett. B **4**, 1009 (1990).
[22]A. I. Ekimov, A. A. Onushchenko, M. E.Raikh, and Al. L. Efros, Zh. Eksp. Teor. Fiz. **90**, 1795 (1986) [Sov. Phys. JETP **63**, 1054 (1986)].
[23]D. A. Kleinman, Phys. Rev. B **28**, 871 (1983).